Biointerphases
A Journal of Biomaterials and Biological Interfaces

ARTICLE

avs.scitation.org/journal/bip

Long-term hydrolytic degradation study of polycaprolactone films and fibers grafted with poly(sodium styrene sulfonate): Mechanism study and cell response

Cite as: Biointerphases 15, 061006 (2020); doi: 10.1116/6.0000429
Submitted: 8 July 2020 · Accepted: 26 October 2020 ·
Published Online: 17 November 2020

Amélie Leroux,[1] Tuan Ngoc Nguyen,[1] André Rangel,[1] Isabelle Cacciapuoti,[2] Delphine Duprez,[3] David G. Castner,[4] and Véronique Migonney[1,a)]

AFFILIATIONS

[1]Laboratory of Biomaterials and Polymers of Specialty, Institut Galilée, Université Sorbonne Paris Nord, CSPBAT UMR CNRS 7244, Villetaneuse 93430, France
[2]Inovarion, Paris 75005, France
[3]Laboratoire de Biologie du Développement, Sorbonne Université, Institut Biologie Paris Seine, CNRS, UMR 7622, INSERM U1156, F75005 Paris, France
[4]National ESCA and Surface Analysis Center for Biomedical Problems (NESAC/Bio), Departments of Bioengineering and Chemical Engineering, University of Washington, Box 351653, Seattle 98195, Washington

Note: This paper is part of the Biointerphases Special Topic Collection on Biointerface Science in Australia 2020 - An issue in celebration of Hans Griesser's career.
[a)]**E-mail:** veronique.migonney@univ-paris13.fr

ABSTRACT

Polycaprolactone (PCL) is a widely used biodegradable polyester for tissue engineering applications when long-term degradation is preferred. In this article, we focused on the analysis of the hydrolytic degradation of virgin and bioactive poly(sodium styrene sulfonate) (pNaSS) functionalized PCL surfaces under simulated physiological conditions (phosphate buffer saline at 25 and 37 °C) for up to 120 weeks with the aim of applying bioactive PCL for ligament tissue engineering. Techniques used to characterize the bulk and surface degradation indicated that PCL was hydrolyzed by a bulk degradation mode with an accelerated degradation—three times increased rate constant—for pNaSS grafted PCL at 37 °C when compared to virgin PCL at 25 °C. The observed degradation mechanism is due to the pNaSS grafting process (oxidation and radical polymerization), which accelerated the degradation until 48 weeks, when a steady state is reached. The PCL surface was altered by pNaSS grafting, introducing hydrophilic sulfonate groups that increase the swelling and smoothing of the surface, which facilitated the degradation. After 48 weeks, pNaSS was largely removed from the surface, and the degradation of virgin and pNaSS grafted surfaces was similar. The cell response of primary fibroblast cells from sheep ligament was consistent with the surface analysis results: a better initial spreading of cells on pNaSS surfaces when compared to virgin surfaces and a tendency to become similar with degradation time. It is worthy to note that during the extended degradation process the surfaces were able to continue inducing better cell spreading and preserve their cell phenotype as shown by collagen gene expressions.

I. INTRODUCTION

Polycaprolactone (PCL) and its copolymers are used in a large number of medical devices and in tissue engineering. The slow degradation rate of PCL allows it to stay several months *in vivo* without significant degradation.[1,2] Additionally, these polymers have many advantages such as (1) flexible mechanical properties;[3–5] (2) ease of processing and fabrication;[6–8] (3) adjustable degradation kinetics by varying crystallinity, molecular weight, structure

geometry (porosity, thickness, etc.);[9–11] and (4) the possibility of being functionalized.[12,13] Currently, there are two common approaches to modify materials to improve their biocompatibility: surface coating or chemical modification/functionalization of the surface. Functionalization of the surface is generally done by the coupling of small molecules via covalent, ionic, or hydrophobic interactions.[14,15] On the other hand, surface coating can be done by depositing the molecule of interest via methods such as plasma spraying, thermal spraying, or electrolytic deposition.[16,17] For hydrophobic polyesters like PCL, these strategies are of particular interest for making their surface more cell adherent and biocompatible to induce favorable interactions with proteins and cells.

For several decades, our laboratory has successfully developed functionalization methods of polymer surfaces introducing carboxylate and/or sulfonate groups for mimicking glycoaminoglycan's functionality and improving cell interaction to improve the biointegration of medical devices.[18–20] In particular, the development of grafting poly(sodium styrene sulfonate) (pNaSS) on polyethylene terephthalate (PET) LARS™ ligaments led to a new generation of biointegrable and bioactive synthetic ligaments.[21–23] The excellent *in vitro* and *in vivo* results in a large animal model (i.e., sheep) demonstrated that the pNaSS grafting provided (1) an increase in the cell adhesion strength;[22] (2) a better morphology of the cells that were more spread out and more homogeneously distributed;[23–25] (3) an increase in type-I collagen production that was accompanied by tissue formation with a better organization;[24,26] (4) an improved osteointegration of prosthesis with the generation of a good bone-implant interface.[27] Based on that, the idea to develop the next generation of synthetic ligaments which could be biointegrable, bioactive, and biodegradable emerged. Thus, pNaSS grafting was extended to PCL surfaces—films, scaffolds, and fibers so far—and bioactivity improvements of those modified materials were studied.[28–30] For the ligament reconstruction application, the impact of the grafting process on mechanical properties as well as the feasibility of a rat implantation model have been assessed and described.[31,32] The first studies on cell response to pNaSS grafted PCL are encouraging; however, one essential question remains for the ligament application: how long does the pNaSS-PCL ligament stay in the body before degrading and are the mechanical properties and bioactivity maintained?

In general, the degradation of poly(α-hydroxy esters) is stimulated by the specific action of water and the phenomena of diffusion and reactions that occur within the material. Two distinct processes are observed: (1) a surface degradation where the diffusion of water in the polymer volume is extremely slow compared to the hydrolytic cleavage reaction and (2) mass degradation where water is able to penetrate through the entire polymer so that random hydrolytic chain splits take place uniformly throughout the matrix.[33] As a poly(α-hydroxy ester), the degradation of PCL is carried out by hydrolysis: the PCL chains are cleaved at the ester bonds, forming carboxyl terminal groups and thereby reducing the size of the molecular chains and yielding water-soluble degradation products such as 6-hydroxylcaproic acid.[11,33–35] When the by-products diffuse into the medium, the degradation, and, therefore, the decrease in the molecular weight throughout the sample are homogeneous, creating a balance between diffusion and hydrolysis reactions.[36] In the case where the by-products do not diffuse into the medium and remain trapped in the mass of the polymer, the presence of the carboxylic acids will catalyze hydrolysis. Under these conditions, a concentration gradient would be present in the material with the rate of degradation of the core of the structure occurring at an exponential rate due to internal autocatalysis.[33]

Many research studies focus on the hydrolytic or enzymatic *in vitro* degradation of PCL copolymers, usually containing polylactic acid, for short- to mid-term applications that are often less than one year.[37–40] Some other studies use accelerated degradation conditions such as extreme *p*H or UV irradiation.[41,42] Predictable mathematic models have also been developed specifically for polyester degradation.[43,44] Nevertheless, a very few articles focused on the long-term (i.e., >1 yr) hydrolytic degradation of pure PCL in a saline solution at *p*H 7.4 and 37 °C.[45] Moreover, although the degradation of some coated-PCL surfaces can be found in the literature,[46–49] a few studies investigated the degradation of functionalized-PCL surfaces.[50,51] This article has two main objectives: (1) investigate the long-term hydrolytic degradation study of two PCL structures—films with a spherulite structure and fiber bundles with a shish-kebab structure—at two degradation temperatures (25 and 37 °C) in saline solution and (2) evaluate the impact of functionalization by radical grafting on PCL degradation to investigate the mechanism of degradation for pNaSS-grafted PCL samples. Therefore, the work presented here is organized into three parts: (1) the degradation study to examine what is the mechanism of the hydrolytic degradation of pNaSS grafted PCL and how does pNaSS impact the degradation reaction; (2) the surface analysis of the degraded material; and (3) the biologic behavior of the resulting degraded structures.

II. MATERIALS AND METHODS

A. Sample preparation

1. PCL film spin-coating

PCL films were cast using a spin-coating method. Raw PCL pellets from Sigma-Aldrich (St Quentin Fallavier, France) (sku. 704105, i.e., PC60 Mn = 60 000 g mol^{-1}) were dissolved in dichloromethane solution (30%, w/v) spin-coated for 30 s at 1500 rpm using a SPIN150-v3 SPS. The cast films were then dried overnight at air pressure and room temperature. Using a punch, the cast films were cut into 14-mm diameter disks and placed at 4 °C until further experiments.

2. PCL fiber bundles

20 PCL fibers (diameter 110 ± 15 μm) from Luxilon Industries, Belgium, were placed in a handmade Teflon plate, in which longitudinal and vertical grooves had been dug. The fibers were placed in the vertical grooves and a PCL solution (1.2 g of PC60 dissolved in 2 ml of dichloromethane) was cast in the longitudinal grooves. After overnight evaporation of dichloromethane, the 20 fibers were joined together forming PCL fiber bundles with a nominal length of 30 ± 1 mm.

3. Grafting of poly(sodium styrene sulfonate) (pNaSS) on PCL samples

a. Purification of the NaSS monomer. Sodium 4-vinylbenzenesulfonate salt (sku. 94904, Sigma-Aldrich) was purified

by recrystallization in a mixed solution of ethanol-distilled water (90:10, v:v). Typically, 90 g NaSS was dissolved in 1780 ml of the mixed solvent at 70 °C overnight. The mixture was then filtrated and the filtrate was placed at 4 °C for 48 h. After final filtration, the filter cake (recrystallized NaSS) was collected, vacuum-dried for 6 h at 30 °C, and kept at 4 °C until further experiments.

b. Radical grafting. The PCL films and bundles were functionalized with pNaSS using a grafting "from" technique. 6 PCL samples were placed in 100 ml of distilled water and ozonated either for 20 min (films) or 10 min (bundles) at 30 °C under stirring. Ozone was generated using an ozone generator BMT 802 N (ACW) with a gas pressure of 0.5 bar and an oxygen flow rate of 0.6 l min^{-1}. Next, the ozonated PCL samples were transferred into a degassed aqueous NaSS solution (15%, w/v) under argon and maintained for 3 h at 45 °C under stirring to allow for radical polymerization of the monomer. The grafted samples were extensively washed with distilled water for 48 h and then vacuum-dried.

B. Degradation study design

The degradation of PCL was assessed by immersion in a saline solution (0.5 ± 0.1 mg ml^{-1}) at 25 °C or 37 °C for 2.5 yr in a controlled temperature chamber without light exposure. The buffered saline solution was composed of 0.14 mol l^{-1} NaCl, 0.01 mol l^{-1} Na_2HPO_4, 0.002 mol l^{-1} KH_2PO_4, and 0.05% of NaN_3 to avoid contamination. This solution was renewed every three months and its *p*H was measured until the degradation time points were reached (original *p*H = 7.4). The degradation of grafted and nongrafted PCL samples was evaluated at 0, 2, 4, 12, and 24 weeks and every 24 weeks after that until 120 weeks (2.5 yr).

1. Characterization of degradation evolution

*a. p*H measurements. At each time point and for each condition examined, the solutions from three randomly assigned samples were kept apart and the others were pooled together. The *p*H of those four solutions was measured by a benchtop *p*H-meter (HI 2210, Hanna Instruments, France).

b. Determination of molecular weights. The PCL number average molecular weight (Mn), weight average molecular weight (Mw), and polydispersity index (PDI) were determined by size exclusion chromatography (SEC) analysis using a Shimadzu Prominence instrument LC20AD pump equipped with a SIL-20ACHT autosampler and a Shimadzu RID-10A differential refractive index detector (Shimadzu Europa GmbH, Duisburg, Germany). The PCL films and fibers were dissolved in tetrahydrofuran (ROTISOLV CLHP, Roth Sochiel EURL, Lauterbourg, France) at 5 mg ml^{-1}. The solutions were filtered (45 μm) and eluted through two SEC columns (phenomenex phenogel, Torrance, USA). A conventional calibration curve was generated using a series of narrow polydispersity poly (methyl methacrylate) standards. Three films or fibers samples were analyzed per condition.

c. Differential scanning calorimetry method. Differential scanning calorimetry (DSC) analyses were carried out with a DSC 8000 calorimeter (Perkin Elmer, Waltham, USA) under nitrogen atmosphere. The samples were scanned once from −75 to 100 °C at a heating rate of 10 °C min^{-1}. The glass transition temperature (T_g), melting temperature (T_m), and melting enthalpy (ΔH_m) of the PCL films were determined from the first scan. The glass transition temperature was assessed using the midpoint method (temperature at which the measured curve is equidistant between the upper and lower tangents). The melting temperature was taken at the maximum of the peak. The melting enthalpy was calculated as the melting peak area. The degree of crystallinity (X_c) was calculated according to Eq. (1),

$$X_c = \Delta H_m/\Delta H_{m0} \times 100, \quad (1)$$

where ΔH_{m0} stands for the melting enthalpy of 100% crystalline PCL (ΔH_{m0} = 135.44 J g^{-1}).[52]

d. Mechanical testing. Mechanical assays were performed in a Bose Electroforce 3220 equipment (TA Instruments, USA). Only the PCL fiber bundles were examined. The effective length of samples was set at 10 mm and the stain rate used was 3.6 mm min^{-1}. Stress strain curves until rupture were recorded and Young's modulus E in MPa, elongation ε in %, and the ultimate tensile stress (UTS) in MPa were determined.

e. SEM images. The microtopography of the PCL surface was carried out using a Hitachi TM3000 SEM operating at 15 kV. For PCL films, the two sides of the sample were observed. No specific sample preparation was done.

f. Atomic force microscope. The nano-topography of the PCL surface was studied by atomic force microscopy (AFM) using a MultiMode 8 model (Bruker, Billerica, USA) and the NANOSCOPE ANALYSIS 1.8 software (Bruker). Each PCL sample was analyzed in air at room temperature using the ScanAsyst mode (tapping mode). The tip used was symmetric, 2.5–8 μm height with a spring constant of 0.4 N/m (70 Hz). The cantilever was made from silicon nitride and had a triangular geometry. The regions of interest for scanning were selected based on the view of the sample in the built-in optical microscope on the AFM instrument. Scanning size performed on PCL was 500 × 500 nm^2.

Mean roughness was calculated by Eq. (2),

$$\mathrm{Ra} = \frac{1}{lr}\int_0^{lr} |Z(x)|\, dx, \quad \text{where Ra is arithmetic average (nm).} \quad (2)$$

g. Contact angle measurements. Static solvent contact angles were measured using a DSA10 contact angle measuring system from KRUSS GmbH. A droplet of solvent was suspended from the tip of a microliter syringe supported above the sample stage. The image of the droplet was captured and the contact angle was measured using the DSA drop shape analysis program from KRUSS-PT 100. The contact angle of dH_2O (2 μl) on the surface was recorded 8 s after contact, three measurements were taken, and averaged.

The surface energy (γ_S) was calculated based on Young's equation,

$$\gamma_S = \gamma_L \cos\theta + \gamma_{SL}, \quad (3)$$

where γ_L is the liquid surface free energy in mN m^{-1}; θ is the contact angle in degrees; and γ_{SL} is the solid/liquid interfacial energy in mN m^{-1}.

The extended Fowker's method was used in these calculations,

$$\gamma_1(1+\cos\theta) = 2(\gamma_1^d\gamma_2^d)^{1/2} + 2(\gamma_1^p\gamma_2^p)^{1/2}. \quad (4)$$

Here, water (polar), ethylene glycol (polar), and methylene iodide (nonpolar) were the liquids used.

h. X-ray photoelectron spectrometry (XPS) analysis. All spectra were taken on a Surface Science Instruments S-probe spectrometer that has a monochromatized Al Kα x-ray and a low energy electron flood gun for the charge neutralization of nonconducting samples. The PCL film samples were fastened to the sample holder using a double-sided tape and run as insulators. X-ray spot size for these acquisitions was approximately 800 μm. The pressure in the analytical chamber during spectral acquisition was less than 5×10^{-9} Torr. The pass energy for survey spectra (to calculate composition) was 150 eV, and the pass energy for high resolution scans was 50 eV. The take-off angle (angle between the sample normal and the input axis of the energy analyzer) was approximately 0°. This take-off angle corresponds to a sampling depth of approximately 100 Å. The SERVICE PHYSICS HAWK DATA ANALYSIS software was used to determine peak areas using a linear background, to calculate the elemental compositions from peak areas and to peak fit the high-resolution spectra. The binding energy scales of the high-resolution spectra were calibrated by assigning the lowest binding energy C1s high-resolution peak a binding energy of 285.0 eV. Three spots were analyzed on each sample for determining the elemental composition. Analysis included a survey spectrum, detailed spectra of the Na1s, N1s, S2p, and Si2p peaks, along with a high-resolution spectrum of the C1s peak from one spot on each sample. Due to the geometry of fibers, this analysis could not be performed on PCL bundles.

i. Colorimetric method. The evidence of pNaSS grafting was tested using the toluidine blue colorimetric assay. The method described by Ciobanu *et al*[21] was adapted as follows: an aqueous solution of toluidine blue (Roth Sochiel EURL) was prepared at 5×10^{-4}M and drops of 1M NaOH were slowly added to reach and maintain the *p*H solution value of 10.0 ± 0.1. Samples were immersed in 5 ml of this solution at 30 °C for 6 h and then washed three times in 5 ml of 10^{-3}M NaOH for 5 min. Each sample was placed in aqueous acetic acid solution (50%, v/v)—in 10 ml for films and in 2 ml for fibers—for 24 h at room temperature. The decomplexation solution was analyzed by UV/visible spectroscopy (Perkin Elmer lambda 25 spectrometer, Waltham, USA) at 633 nm. On the grafted surfaces, 1 mol of toluidine blue was assumed to complex 1 mol of the sulfonate group from pNaSS. The grafting rate (*GR*) in mol g^{-1} was then calculated according to Eq. (5),

$$GR = \frac{ODV}{\varepsilon l\, m}, \quad (5)$$

where *OD* is the optical density, *V* is the aqueous acetic acid volume (l), ε is the extinction coefficient of toluidine blue solution (l mol^{-1} cm^{-1}), *l* is the length of the spectrophotometer tank (cm), and *m* is the mass of the PCL films (g). The extinction coefficient was calculated based on a dilution curve using the initial toluidine blue solution.

j. ATR-FTIR analyses. The Fourier-transformed infrared (FTIR) spectra, recorded in attenuated total reflection (ATR), were obtained using a Perkin Elmer Spectrum Two spectrometer. The PCL films were uniformly pressed against a diamond crystal and for each surface, 128 scans were acquired from 4000 to 400 cm^{-1} at a resolution of 2 cm^{-1}.

2. Cell culture analyses

a. Preparation of the samples for cell culture. Prior to experiments, all PCL films were packaged and sterilized as follows: 3× washing (3 h in 0.15M NaCl), 20 min in 70% ethanol, 10 min in ultra-pure water, and 15 min UV irradiation (both sides of the samples). All steps were performed under stirring. The PCL films were kept in sterile PBS solution at −20 °C until further experiments. The samples were then slowly defrozen and placed overnight at 37 °C under 5% CO_2 in a cell culture medium (DMEM, Gibco) without supplementation followed by an overnight incubation at 37 °C under 5% CO_2 in cell culture medium supplemented with 10% FBS.

b. Isolation and culture of primary sheep anterior cruciate ligament fibroblasts. Anterior cruciate ligaments (ACLs) were isolated from one sheep (2-yr-old female Merino sheep free of degenerative joint disease, ~60 kg) in accordance with the German legislation on protection of animals and the NIH Guidelines for the Care and Use of Laboratory Animals (NIH Publication 85-23, Rev. 1985) and as approved by the local governmental animal care committee.[53] Tissues were cut into small pieces of 1–2 mm^2, washed three times in DPBS, and incubated in a 0.1% (w/v) collagenase (Sigma-Aldrich) for 6 h at 37 °C under 5% CO_2. The mixture solution was centrifuged 3 min at 1500 rpm. The supernatant was withdrawn and the clot resuspended in DMEM complemented with 10% bovine calf serum (BCS) (Sigma-Aldrich), 1% penicillin-streptomycin (Gibco), and 1% L-glutamine (Gibco). The primary sheep ACL (sACL) fibroblasts were maintained in T-75 flasks until confluence was reached. pNaSS-grafted and nongrafted PCL films were placed on the bottom of a 24-well plate using Teflon inserts. The cells were then seeded at a density of 5×10^4 cells/well and cultured at 37 °C under 5% CO_2 over the time of the experiment.

c. Cell viability. PCL films were chemically degraded for 1 month in 2 ml of HCl solution (1 mol l^{-1}) at 40 °C. The macroscopic degraded pieces of PCL were collected and analyzed by SEC, while the solvent suspensions were equilibrated to *p*H 7 with

NaOH (1 mol l^{-1}). After sterilization under 0.22 μm filtration, the solutions containing the PCL degraded products were put in contact with sACL fibroblasts for 24 h in DMEM complemented with 10% serum (dilution factor of 1/5).

The medium was removed and 500 μl of MTT solution (Sigma, Saint Louis, MO, USA) at a final concentration of 1 mg ml^{-1} diluted in a fresh culture medium without phenol red was incubated for 4 h at 37 °C. The supernatant was then discarded and 350 μl of DMSO was added to each well for 10 min at room temperature. Each well was thoroughly mixed and the absorbance was read at 570 nm. The percentage of live cells in the presence of PCL degraded products was calculated using a calibration curve between the number of cells and the corresponding absorbance.

d. Histological and fluorescence analyses. sACL fibroblasts were harvested, fixed for 30 min with 4% formaldehyde, and rinsed twice with PBS. For histological analyses (hematoxylin and eosin—H&E—staining), hematoxylin (Carl Roth GmbH, Karlsruhe, Germany) was first added to each well for 10 min. The wells were then washed once with distilled water and a solution of 1% HCl was briefly added. Prewarmed water (60 °C) was added for 4 min, followed by the addition of hematoxylin for 3 min, removal, and washing once with distilled water. Eosin (Carl Roth GmbH) was then incubated for 2 min and extensively washed with distilled water. Stained samples were kept at 4 °C until observation under a light microscope (Olympus BX 45, Hamburg, Germany).

For fluorescence analyses, the cells were fixed and the samples washed once with PBS and once with 3% bovine serum albumin (BSA)/PBS (Acros Organics, Geel, Belgium). The cells were then permeabilized with 0.1% Triton-X 100 in PBS for 5 min at room temperature. After two washes in PBS, the samples were incubated in 3% BSA/PBS for 1 h at room temperature. The cells were then incubated with Fluorescein Phalloidin (FITC, Molecular probes, Eugene, USA) at 1:40 in 1% BSA/PBS for 1 h at room temperature in the dark. After two washes in PBS, 2% 4′,6-diamidino-2-phenylindole (DAPI) dissolved in distilled water was added for 10 min at room temperature. The samples were stored in distilled water at 4 °C until observation under a fluorescent microscope (Olympus CKX41).

e. Total RNA extraction and real-time q-PCR analyses. Sheep ACL cells were cultured for 7 days on grafted or nongrafted PCL films, which have been subjected to 24, 48, 84, and 96 weeks of degradation. For each condition, total RNA was isolated using the RNeasy mini kit according to the manufacturer's protocol (Qiagen, Hilden, Germany). For each experimental condition, 100 ng RNA was reverse-transcribed using the high capacity retrotranscription kit (Applied Biosystems, Thermo Fisher Scientific). Quantitative PCR was performed using a SYBR Green PCR Master Mix (Applied Biosystems, Thermo Fisher Scientific) using the following primers (Sigma-Aldrich, Merck), COL1A1 (type-I collagen α 1), COL2A1 (type-II collagen α 1), and COL3A1 (type-III collagen α 1), which are listed in Table I. COL1A1 and COL3A1 identify ligament collagens, while COL2A1 identifies cartilage collagen. We used GAPDH as a housekeeping gene for internal control. All primers were used at the 3 μM final concentration. The threshold cycle (Ct) value for each gene of interest was measured for each amplified sample by using the STEPONE software (Applied Biosystems, Thermo Fisher Scientific) and was normalized to GAPDH expression. The relative mRNA levels were calculated using the 2−ΔΔCt method described by Livak and Schmittgen.[54] The ΔCt values were obtained by calculating the differences: Ct (gene of interest)−Ct(housekeeping gene) in each sample. We obtained the ΔΔCt values by calculating the differences between ΔCt(Experiment) and the average of ΔCt(control) values. For relative mRNA level analysis, the COL2A1 values of nongrafted and nondegraded PCL were used as control and normalized to 1.

TABLE I. Primers used for q-PCR.

COL1A1	Forward 5′-CGTGATCTGCGACGAACTTA-3′
	Reverse 5′-TCCAGGAAGTCCAGGTTGTC-3′
COL2A1	Forward 5′-CAACCAGGACCAAAGGGACA-3′
	Reverse 5′-GTCACCACGATCACCTCTGG-3′
COL3A1	Forward 5′-CCGTGCCAAATATGCGTCTG-3′
	Reverse 5′-GTGGGCAAACTGCACAACAT-3′
GAPDH	Forward 5′-ACAGTCAAGGCAGAGAACGG-3′
	Reverse 5′-CCAGCATCACCCCACTTGAT-3′

f. Statistical analysis. All the bulk analyses were carried out on three independent samples, all the surface analyses were carried out on three different spots on one sample, all the biological experiments were carried out using one to three samples per condition. Statistical analyses were performed using ANOVA with $p \leq 0.05$ considered statistically significant.

III. RESULTS

A. Bulk analysis of degraded material

1. pH measurement

No significant change was found in the *p*H of the solution after 120 weeks of degradation ($p > 0.05$), the *p*H never deviated more than 3% from the original 7.4 *p*H value for the different conditions studied [see Fig. 1 for films and Fig. S1 (Ref. 62) in the supplementary material for fibers].

2. Molecular weight

The monitoring of the molecular weights over time revealed different degradation processes, depending on the sample type and experimental conditions [cf. Fig. 2(a)]. For the nongrafted samples, M_n decreased slowly over the first year (i.e., 48 weeks) and then reached a plateau. After 2.5 yr of degradation (i.e., 120 weeks), the nongrafted PCL film molecular weight decreased by 11.4 ± 2.6% ($p \leq 0.05$). The PDI of the nongrafted films remained constant over the 2.5 yr period with a value of 1.29 ± 0.02 [cf. Fig. 2(b)]. These trends in M_n and PDI were similar whether degradation occurred at 25 or 37 °C, even if the loss in molecular weight was slightly increased at the higher temperature ($p \leq 0.05$).

For the grafted samples, the degradation kinetics was significantly different ($p \leq 0.05$). First, the molecular weight loss depended on the degradation temperature of 25 or 37 °C. At 25 °C,

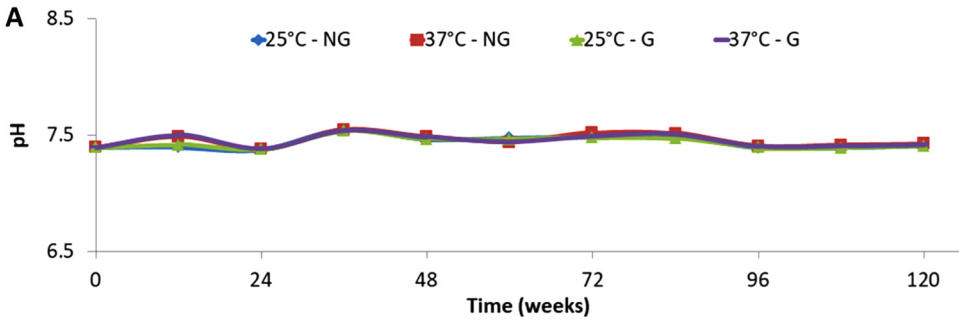

FIG. 1. *p*H variation of the saline solution used for the degradation of PCL films.

the molecular weight loss of the pNaSS grafted samples was 8.0 ± 1.4% ($p \leq 0.05$) after the first 6 months, increased to 30.7 ± 6.2% loss ($p \leq 0.05$) after 1 yr and finally stabilized at 40.1 ± 2.7% loss ($p \leq 0.05$) after 1.5 yr [cf. Fig. 2(a)]. The PDI increased as M_n decreased, reaching a value of 1.49 ± 0.10 ($p \leq 0.05$) after 1.5 yr of degradation [cf. Fig. 2(b)]. The degradation of the pNaSS grafted sample was accelerated at 37 °C compared to 25 °C. After 6 months, the molecular weight decrease was 27.7 ± 0.2% ($p \leq 0.05$) and reached a plateau at 1 yr corresponding to 76.5 ± 6.3% of molecular weight loss ($p \leq 0.05$) [cf. Fig. 2(a)]. The PDI variation for this sample was different from the other conditions, for the first 6 months (i.e., 24 weeks), and the PDI was stable at 1.35 ± 0.06 and then it increased to 2.30 ± 0.15 ($p \leq 0.05$) after 1 yr of degradation [cf. Fig. 2(b)].

Similar trends, but to a lesser extent, were observed for the degradation of the PCL bundles [cf. Fig. S2 (Ref. 62) in the supplementary material]. The initial molecular weight of the fibers was higher than the films (i.e., 74 317 ± 412 g mol^{-1} for the fibers versus 60 438 ± 203 g mol^{-1} for the films), which slowed down the degradation process of the fiber bundles.

3. DSC

For all conditions, the degradation of the films was linked to increases in crystallinity and melting temperature (T_f). Although, it occurs differently at 25 °C compared to 37 °C.

The crystallinity of the nongrafted samples degraded at 25 °C for 120 weeks increased by 4.4% ($p > 0.05$), whereas the crystallinity of the grafted samples at 25 °C for 120 weeks increased by 12.8% ($p > 0.05$). After 120 weeks at 37 °C, there was no difference between grafted and nongrafted samples, which had crystallinity increases of 16.1% ($p \leq 0.05$). The increase in crystallinity can be observed by the size of the melting peak in the thermograms (Fig. 3).

The degradation temperature significantly influenced T_f, causing a shift in the melting peak. An increase in 6% ($p \leq 0.005$) was observed when films were degraded at 25 °C (from $T_f = 60.52 \pm 0.58$ °C to $T_f = 64.41 \pm 0.02$ °C) compared to an increase of 8.8% ($p \leq 0.005$) when degraded at 37 °C (from $T_f = 60.52 \pm 0.58$ °C to $T_f = 66.34 \pm 0.20$ °C) (see Fig. 3).

4. Mechanical—Fiber samples

Tensile tests were carried out over 2.5 yr of degradation on the PCL bundles (20 fibers) to follow the evolution of crucial characteristics in the mechanical performance of the studied materials. After only 2 weeks of degradation, all samples exhibited a reduction of Young's modulus values ($p > 0.05$), the reduction being more prominent for nongrafted samples, which reached the same mean value of the grafted samples after 4 weeks of degradation (i.e., $E \approx 1075$ MPa) [cf. Fig. 4(a)]. Those values remained relatively stable for the next 20 weeks and then progressively decreased until 72 weeks of degradation. From 72 to 120 weeks, Young's modulus is once again relatively stable.

Similarly, after the first 2 weeks of degradation, the elastic strain for grafted and nongrafted samples converge to similar values (i.e., $\varepsilon \approx 14\%$, $p > 0.05$). These values remained relatively constant for the next 10 weeks and then experienced a substantial increase after 24 weeks of degradation ($p \leq 0.005$). After 24 weeks, the elastic strain of both samples degraded at 25 °C remained fairly constant. In contrast, the elastic strain of both samples degraded at 37 °C decreased. The elastic strain decrease of the

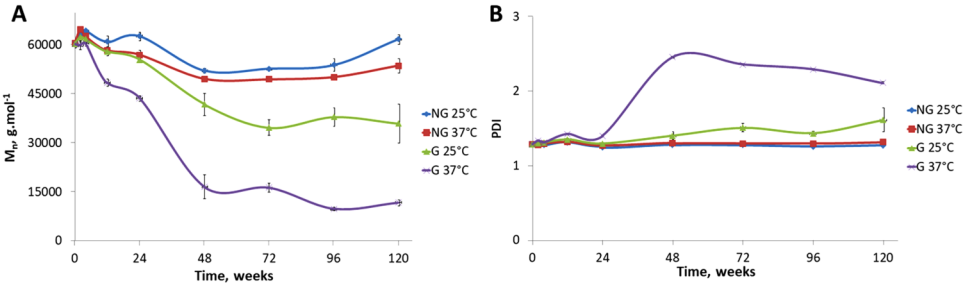

FIG. 2. SEC analysis results. (a) Evolution of M_n over degradation time, (b) evolution of PDI over degradation time.

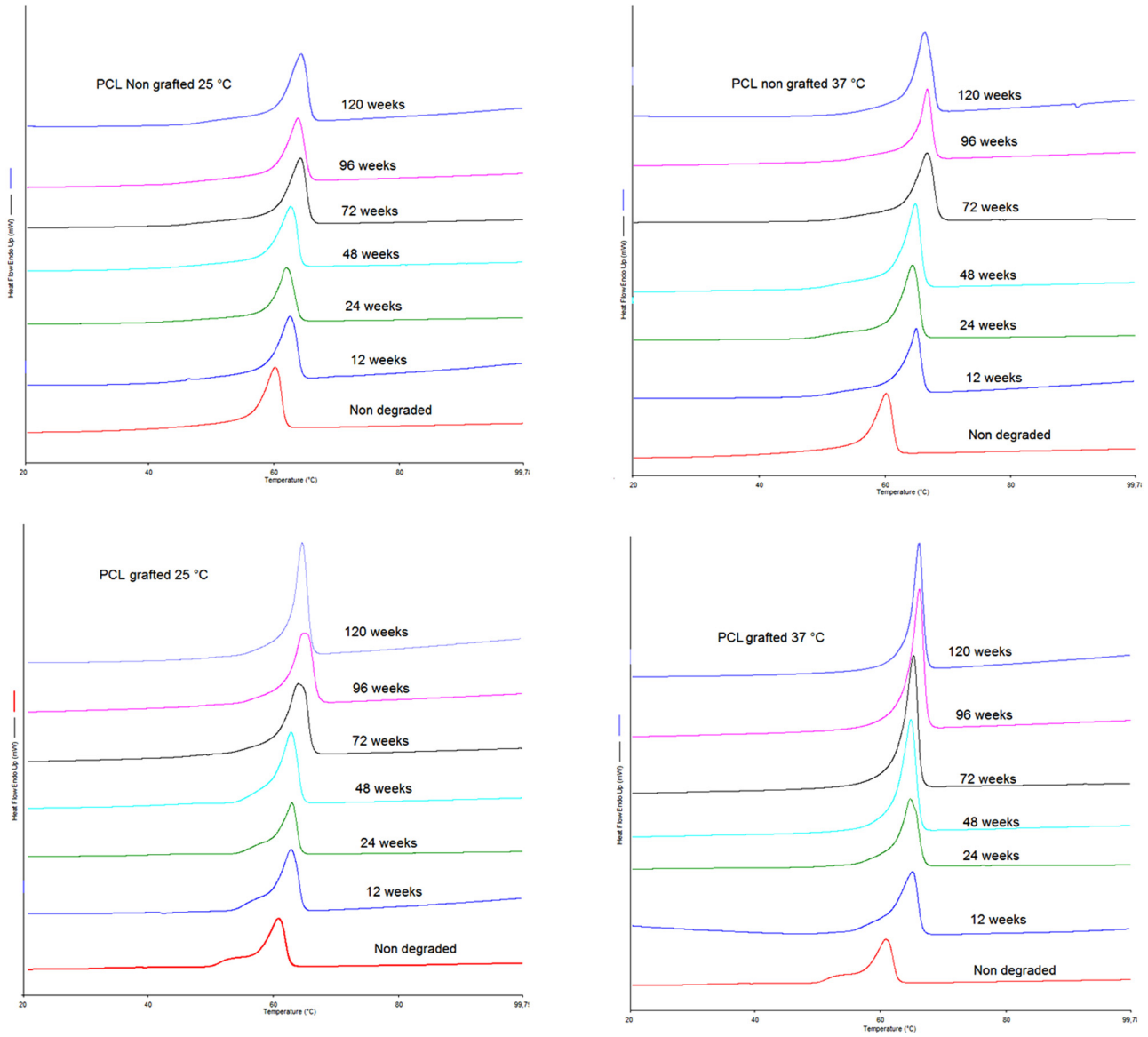

FIG. 3. DSC thermograms of the first heat for nongrafted and grafted PCL films degraded for 0, 12, 24, 48, 72, 96, and 120 weeks degradation at 25 °C and 37 °C.

grafted sample began at 24 weeks and was more intense after 72 weeks, while for the nongrafted sample, it did not begin until 72 weeks [Fig. 4(b)].

The behavior of these two parameters can be associated with the weakening of the material by the degradation process. The reduction of the ultimate stress also showed that the grafted samples degraded more rapidly at 37 °C ($p \leq 0.05$) [cf. Fig. 5(a)]. Figure 5(b) shows the stress-strain profiles for the grafted sample degraded at 37 °C along with the evolution of ultimate stress for all samples as a function of degradation time.

B. Surface analysis of degraded samples

1. Microtopography

PCL spin-coated films presented a microstructure composed by amorphous and crystalline parts arranged in spherulites structures (see Fig. 6). pNaSS grafting did not change the size of the spherulites nor their proportion in the films, but some straight lines appeared. After 24 weeks of degradation, the nongrafted samples lost their amorphous part (see circles in Fig. 6), while the grafted films started to present additional cracks in the crystalline

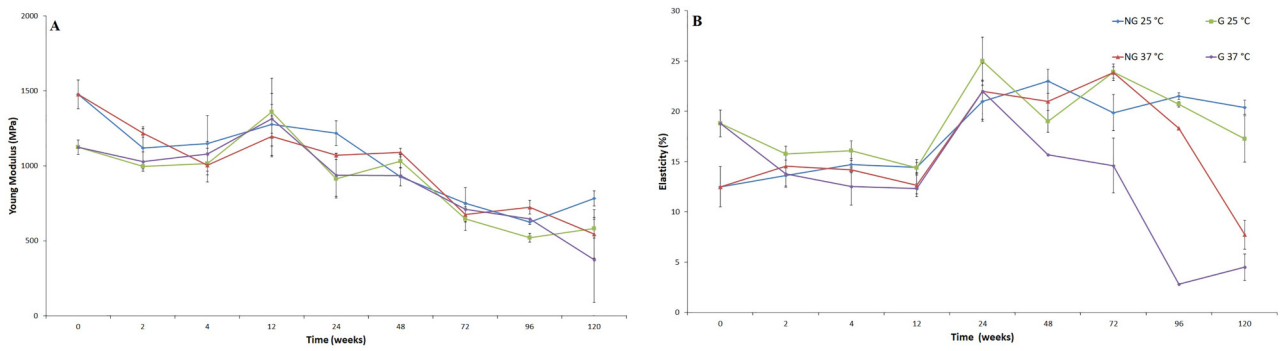

FIG. 4. (a) Evolution of Young's modulus for PCL bundles over degradation time; (b) evolution of elastic strain percentage for PCL bundles over degradation time.

part (see arrows in Fig. 6). At 48- and 72 weeks of degradation, we observed a rearrangement of the structure with an increase in the spherulite size. The grafted films presented some microscopic holes between spherulites and a lot of cracks localized in the germination points (see, respectively, stars and arrows in Fig. 6). At 96 weeks, the spherulites returned to their initial size. The first layer of the grafted films started to disappear and films became very brittle. It was less obvious on the nongrafted samples, where almost no cracks of the crystalline part appeared over degradation time. At 120 weeks of degradation, the films recovered a homogeneous microtopography that looks very crystalline with the grafted films still presenting a lot of cracks in this crystalline structure (see arrows in Fig. 6).

The same observations were made on nongrafted and grafted films when degraded at 25 °C.

On PCL fiber bundles, due to the spinning process, we assumed that the initial structure was organized in a shish-kebab pattern. The fiber microstructure observed by SEM did not show any differences between nongrafted and grafted surfaces, or between 25 °C- and 37 °C-degradation. The only observation was that fibers looked "rougher" (casting ridges accentuated) with degradation time and 120 weeks of degradation at 37 °C was required to start observing holes at the surface [see Fig. S3 (Ref. 62) in the supplementary material].

2. Nanotopography

AFM analysis demonstrated a difference in the surface topography between nongrafted and pNaSS grafted surfaces. The increase in image mean roughness (Ra) going from 2.85 nm at 0 weeks of degradation to 14.3 nm at 120 weeks of degradation ($p \leq 0.05$) demonstrated that the nongrafted surface became rougher after long term degradation. The degradation, represented by a roughness increase, also occurred with grafted films but was significant only after at 120 weeks of degradation (Ra = 8.4 nm, $p \leq 0.05$) (see Fig. 7).

The similar phenomenon happened with PCL fibers under the same conditions [see Fig. S4 (Ref. 62) in the supplementary material].

3. Contact angle measurement

The nongrafted PCL film samples degraded at 25 and 37 °C, as well as the pNaSS grafted films degraded at 25 °C, did not exhibit a significant change in their water contact angle measurements with degradation time ($p \leq 0.05$). In contrast, the pNaSS grafted films degraded over 120 weeks at 37 °C displayed a

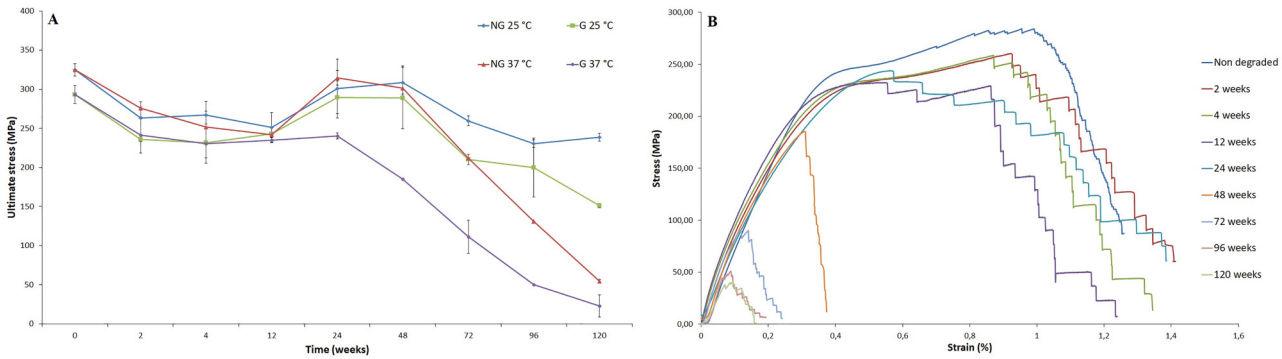

FIG. 5. (a) Evolution of the ultimate stress with degradation time; (b) strain stress curves for grafted samples degraded at 37 °C.

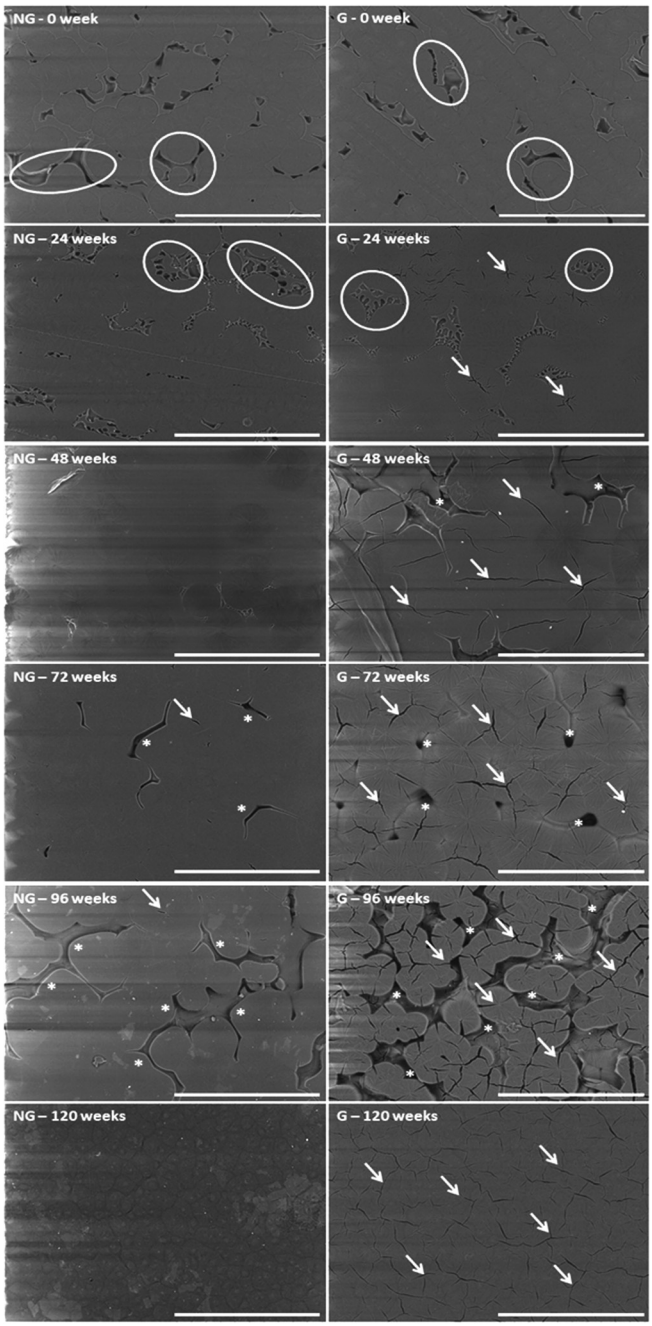

FIG. 6. SEM images of nongrafted (NG) and pNaSS grafted (G) PCL films degraded at 37 °C for 0, 24, 48, 72, 96, and 120 weeks. Scale bar = 300 μm. Legend: circle = amorphous region; arrow = crack; and star = hole.

significant decrease in the water contact angle going from 66.6 ± 0.9 to 54.0 ± 4.3 (28.1% decrease, $p \leq 0.05$). This decrease is consistent with an increase in the surface hydrophilicity with degradation (Table II).

The surface energy, calculated according to Eq. (3) (see in Tables S1 and S2[62] for contact angle results with ethylene glycol and diiodomethane), was higher on the grafted than on the nongrafted films due to the presence of sulfonate groups on the surface of the grafted films (see Table III). The degradation of the PCL films did not significantly impact the surface energy ($p > 0.05$) and retained the initial difference observed between nongrafted and grafted samples.

Additionally, the polar energy of nongrafted films was not changed by the degradation process, but an increase of this energy to 8.8 ± 1.6 mN m^{-1} was observed for the grafted samples degraded at 37 °C for 120 weeks (Table IV).

4. XPS analysis

The XPS analysis provided information about the degradation of the PCL films in the outer ~100 Å of the samples. For the nongrafted samples degraded at 37 °C, no significant variation of the carbon species concentrations was observed in the first 72 weeks of degradation, but at 96 weeks of degradation (i.e., 2 yr) an increase of 42% of the C—O bonds was observed [cf. Fig. 8(a)]. Interestingly, the XPS analysis on the grafted PCL films presented the same increase of 42% in C—O bonds after 96 weeks of degradation but with a more continual increase with degradation time (11% and 17% after 24 and 72 weeks of degradation, respectively) [cf. Fig. 8(b)].

The XPS determined atomic concentrations for all degraded PCL films were similar, but trace amounts of sulfur (~0.2 atomic percent) were detected on the grafted PCL films after degradation (see Table V). The grafted samples prior to degradation exhibited a significantly different XPS elemental composition, due to the presence of the pNaSS film (increased sulfur, increased oxygen, and decreased carbon). The colorimetric method could not be used to measure the amount of the grafted pNaSS on the degraded samples due to a significant increase in the nonspecific coloration of the degraded damaged surfaces ($p \leq 0.05$, see results on nongrafted samples in Table V). XPS showed a decrease of the sulfur concentration (1.8 to 0.2 at. % sulfur) upon degradation (see Table V).

5. Fourier transform infrared spectra

During the degradation process, the 1720 cm^{-1} [γ(C═O)] and 1167 cm^{-1} peaks [ν_{as}(C—O)] decreased (under 0.6% of transmittance—see the decrease in the red intensity on color maps) after 84 weeks for the nongrafted PCL film (see Fig. 9). The increase in the number of C—OH and COOH groups caused the significant decrease in these peaks. That phenomenon is related to the increased percentage in —CO bonds in the XPS C1s spectra as degradation proceeded.

The increase in alcohol and acid groups on polymer chain could be observed by a shift of the C—O peak position.[55] By breaking the C—O—C bond to form a C—OH bond, the C—O stretch changed, leading to the blue-shift of the C—O peak from 1160 to 1180 cm^{-1} [see Fig. 10(a)]. The decrease in transmittance and the blue-shift of C—O peaks are important keys to predict the surface degradation. Following the sulfonate groups with degradation time, by monitoring the 1008 cm^{-1} peak, revealed the presence of sulfonate groups even after 96 weeks of degradation. However, this peak lost intensity as the degradation process proceeded, as observed in the XPS analysis [see Fig. 10(b)].

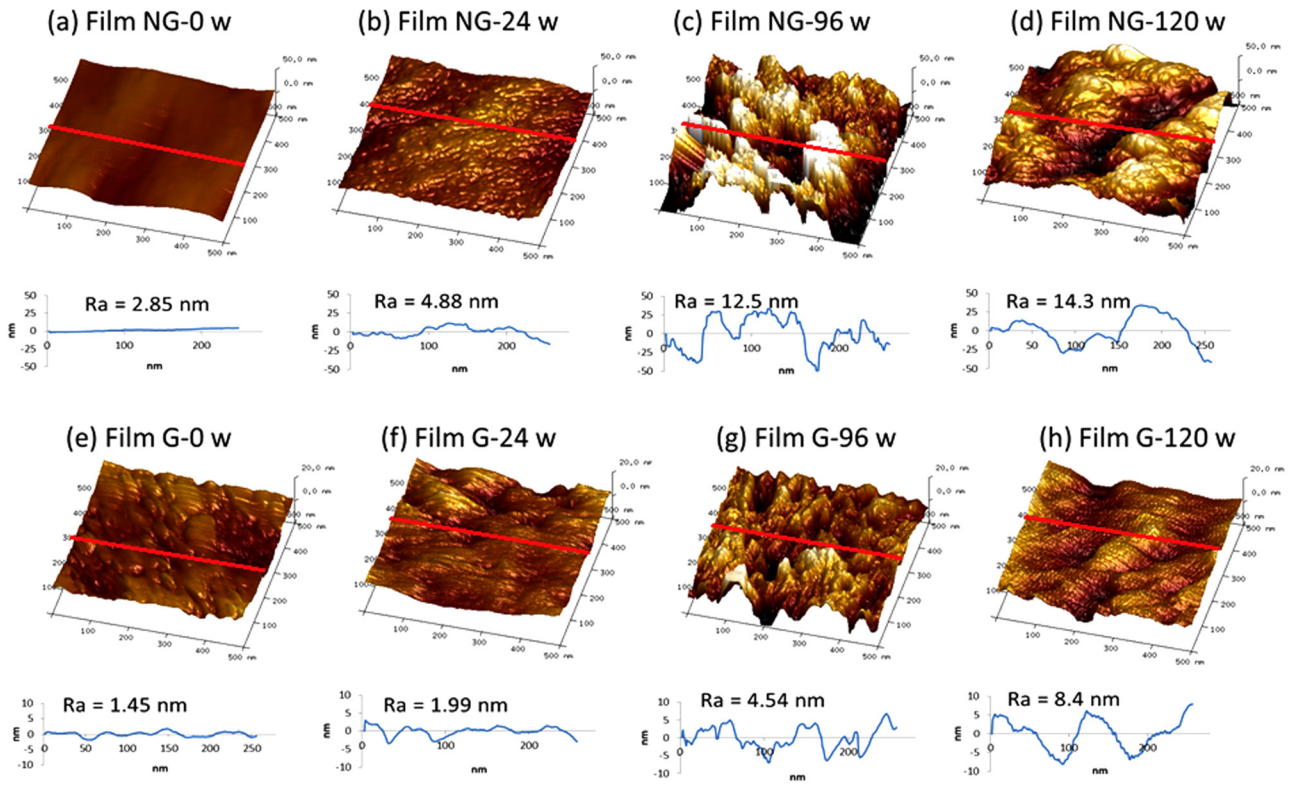

FIG. 7. Nanotopography of nongrafted (NG) and grafted (G) PCL films degraded at 37 °C: (a) nondegraded NG film, (b) 24 wt. % degraded NG film, (c) 96 wt. % degraded NG film, (d) 120 wt. % degraded NG film, (e) nondegraded G film, (f) 24 wt. % degraded G film, (g) 96 wt. % degraded G film, (h) 120 wt. % degraded G film. Scan size: 500 × 500 nm^2, the roughness diagram was measured over the red line.

C. Impact on biologic behavior

1. Cell viability

A SEC analysis of the macroscopic pieces of PCL chemically degraded revealed an M_n of 11 228 ± 2481 g mol^{-1} independent of grafting. This molecular weight was similar to that observed for grafted-PCL films naturally degraded for 2.5 yr at 37 °C. The solution from the chemical degradation was then put in contact to cells to study the cytotoxicity effect of the PCL degradation products. The percentage of live cells in the degradation solutions from the nongrafted films and grafted films was 100.01 ± 0.12% and 100.26 ± 0.22%, respectively ($p > 0.05$).

2. Cell morphology

The fluorescence observations showed that primary ACL cells were better spread on the grafted PCL films compared to the

TABLE II. Water contact angle on PCL films degraded over time at 25 and 37 °C.

	Contact angle (deg) water			
	Degradation at 25 °C		Degradation at 37 °C	
Time (weeks)	Nongrafted	Grafted	Nongrafted	Grafted
0	77.0 ± 0.5	66.6 ± 0.9	77.0 ± 0.5	66.6 ± 0.9
12	77.4 ± 1.8	64.2 ± 5.1	68.3 ± 1.1	70.2 ± 3.6
24	77.9 ± 1.4	71.1 ± 3.0	76.0 ± 3.2	68.9 ± 0.6
48	76.5 ± 0.9	66.3 ± 6.9	72.3 ± 3.8	76.1 ± 2.6
72	71.3 ± 7.6	73.1 ± 4.8	82.1 ± 0.3	63.2 ± 0.6
96	71.4 ± 1.6	66.2 ± 0.2	75.4 ± 2.5	50.1 ± 3.1
120	72.8 ± 2.0	68.3 ± 2.3	73.0 ± 1.6	54.0 ± 4.3

TABLE III. Surface energy (total) of nongrafted and grafted films degraded at 25 and 37 °C.

	γ_S (mN m^{-1})			
	Degradation at 25 °C		Degradation at 37 °C	
Time (weeks)	Nongrafted	Grafted	Nongrafted	Grafted
0	40.6 ± 0.3	44.5 ± 0.5	40.6 ± 0.3	44.5 ± 0.5
12	44.8 ± 1.1	46.0 ± 1.6	45.9 ± 0.9	46.9 ± 0.3
48	43.4 ± 0.4	45.9 ± 0.9	42.2 ± 1.4	43.9 ± 0.5
72	43.2 ± 0.5	46.4 ± 1.9	43.0 ± 0.3	46.0 ± 1.4
96	43.5 ± 1.6	45.6 ± 0.6	42.8 ± 0.7	52.4 ± 1.1
120	36.2 ± 2.6	47.0 ± 3.2	42.6 ± 0.9	53.2 ± 2.5

TABLE IV. Polar fraction of nongrafted and grafted films degraded at 25 and 37 °C.

	γ^P (mN m^{-1})			
	Degradation at 25 °C		Degradation at 37 °C	
Time (weeks)	Nongrafted	Grafted	Nongrafted	Grafted
0	2.4 ± 0.1	3.7 ± 0.2	2.4 ± 0.1	3.7 ± 0.2
12	1.6 ± 0.3	4.8 ± 0.5	4.1 ± 0.2	3.1 ± 0.3
48	2.1 ± 0.3	4.9 ± 0.6	2.8 ± 1.2	2.2 ± 0.4
72	2.7 ± 0.1	3.6 ± 1.3	1.0 ± 0.1	4.9 ± 0.5
96	3.5 ± 0.5	4.5 ± 0.2	3.3 ± 0.6	9.4 ± 0.9
120	2.8 ± 0.8	5.1 ± 1.1	3.7 ± 0.5	8.8 ± 1.6

nongrafted PCL films (see Fig. 11). Although the number of nuclei did not seem to differ between the two conditions, the actin cytoskeleton was more developed for the cells on the grafted samples. As the degradation of PCL proceeded at 37 °C, the examination of the fluorescence images became more complicated due to nonspecific attachment of the fluorochromes, but it appeared the difference observed between the nondegraded nongrafted and grafted films was maintained during the degradation process. These observations were confirmed with the eosin/hematoxylin staining at selected time points. The same results were observed for the films degraded at 25 °C.

3. Gene expression

The expression of collagen genes, associated with the fibroblast/ligament phenotype, COL1A1 and COL3A1, was not modified in sheep ACL cells cultured on grafted or nongrafted PCL films subjected to degradation over the 96-wk time period (see Fig. 12). The expression of COL2A1 gene, a specific marker of cartilage, was not detected in sheep ACL cells at any of the experimental conditions, indicating that ACL cells did not differentiate into cartilage when cultured on degraded PCL. This molecular analysis showed that the PCL degradation process did not affect the ligament phenotype of ACL cells.

IV. DISCUSSION

A. Bulk analysis of material degradation

The natural degradation of PCL samples—films and fiber bundles—with or without a grafted bioactive polymer—was studied at two temperatures (i.e., 25 and 37 °C) for 120 weeks in a saline solution. No change in the solution *p*H was observed, indicating that the release of acid species from the PCL degradation could not be detected.

The hydrolysis degradation process of the PCL polymeric chains appeared to be different when the surface was grafted with pNaSS. In particular, after 6 months, the grafted samples exhibited accelerated molecular weight losses and increased PDIs. It should be noted that during the first 6 months, the SEC determined molecular weights for 37 °C-degraded grafted samples were only slightly lower than the other samples and that the PDI results demonstrated that the PCL chains were cut homogeneously during this time. After 6 months of degradation, the SEC results showed a drastic drop of M_n and a significant increase of PDI. These effects were accentuated at the higher degradation temperature. In all conditions, degradation increased the global crystallinity of the polymer, as determined by the increased melting temperature detected during the first scan of DSC for both films and fiber bundles. This increase in crystallinity was due to the preferential loss of the amorphous component in the films.

Although no significant M_n variation has been noticed, mechanical properties under rupture load on nongrafted and pNaSS grafted PCL bundles reached the same level after 2–4 weeks of natural degradation. This fact can be explained by two different phenomena: (1) the reduction of nongrafted sample's Young's modulus can be linked to the structure modification when in an aqueous environment, (2) the temperature of the degradation

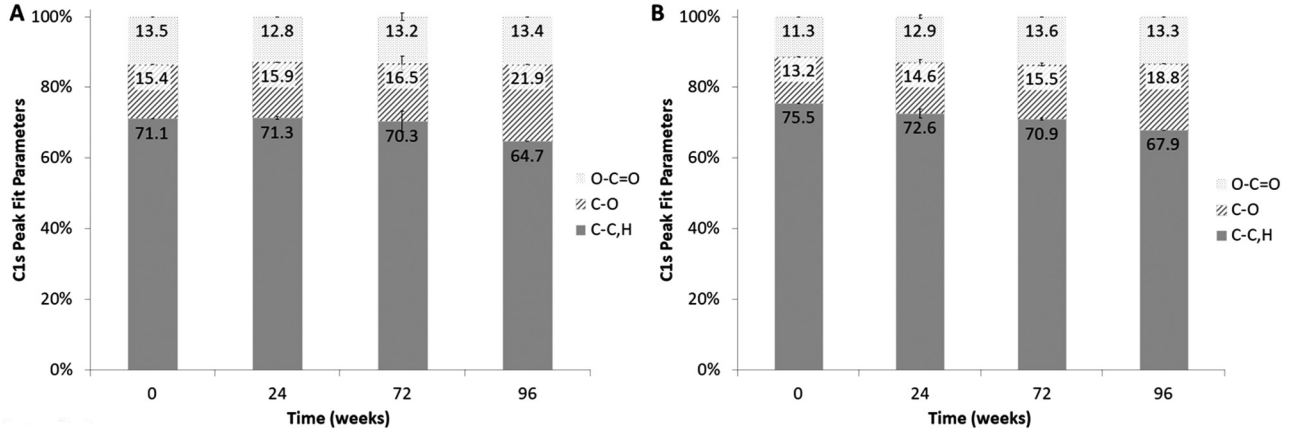

FIG. 8. C1s peak fit parameters—percentages of atomic bonds for (a) nongrafted PCL films degraded overtime at 37 °C and (b) grafted PCL films degraded overtime at 37 °C.

TABLE V. Grafting rates (GRs) determined according to Eq. (5) (see Sec. II) and surface concentration (XPS atomic percent) for nongrafted (NG) and grafted (G) PCL films degraded at 37 °C for 0, 24, 72, or 96 weeks.

	GR (μmol g^{-1})		Atomic concentration (%)					
	Before degradation	After degradation	C 1s	O 1s	S 2p	Na 1s	N 1s	Si 2p
NG—0 wk	0.70 ± 0.27	-	72.1 ± 0.9	22.7 ± 0.9	-	-	-	3.4 ± 0.1
NG—24 weeks	1.05 ± 0.45	0.99 ± 0.35	76.3 ± 0.4	21.9 ± 0.4	-	0.2 ± 0.1	-	1.7 ± 0.2
NG—72 weeks	0.47 ± 0.40	2.13 ± 0.70	76.8 ± 0.9	20.2 ± 0.9	0.1 ± 0.0	0.3 ± 0.1	1.5 ± 0.6	1.1 ± 0.3
NG—96 weeks	0.30 ± 0.12	7.26 ± 0.96	73.1 ± 0.8	22.7 ± 0.7	0.1 ± 0.1	0.6 ± 0.1	2.3 ± 0.2	1.2 ± 0.1
G—0 weeks	10.5 ± 0.06	-	61.4 ± 0.7	29.6 ± 0.8	1.8 ± 0.1	0.9 ± 0.1	-	1.5 ± 0.4
G—24 weeks	8.51 ± 0.81	41.30 ± 5.46	74.5 ± 0.0	22.5 ± 0.4	0.3 ± 0.0	0.6 ± 0.0	-	2.2 ± 0.4
G—72 weeks	4.79 ± 0.87	96.70 ± 3.16	77.3 ± 0.4	21.1 ± 0.4	0.2 ± 0.1	0.5 ± 0.0	0.5 ± 0.2	0.5 ± 0.2
G—96 weeks	3.31 ± 1.34	156.00 ± 9.57	75.5 ± 0.9	22.9 ± 0.9	0.2 ± 0.0	0.7 ± 0.1	0.4 ± 0.2	0.3 ± 0.1

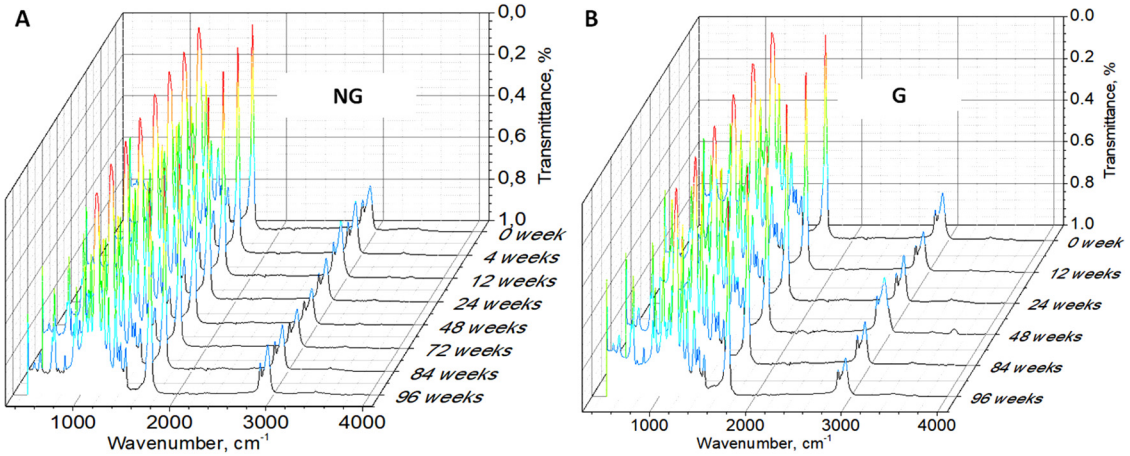

FIG. 9. Fourier transform infrared spectra of nongrafted (a) and grafted (b) PCL films degraded at 37 °C over time.

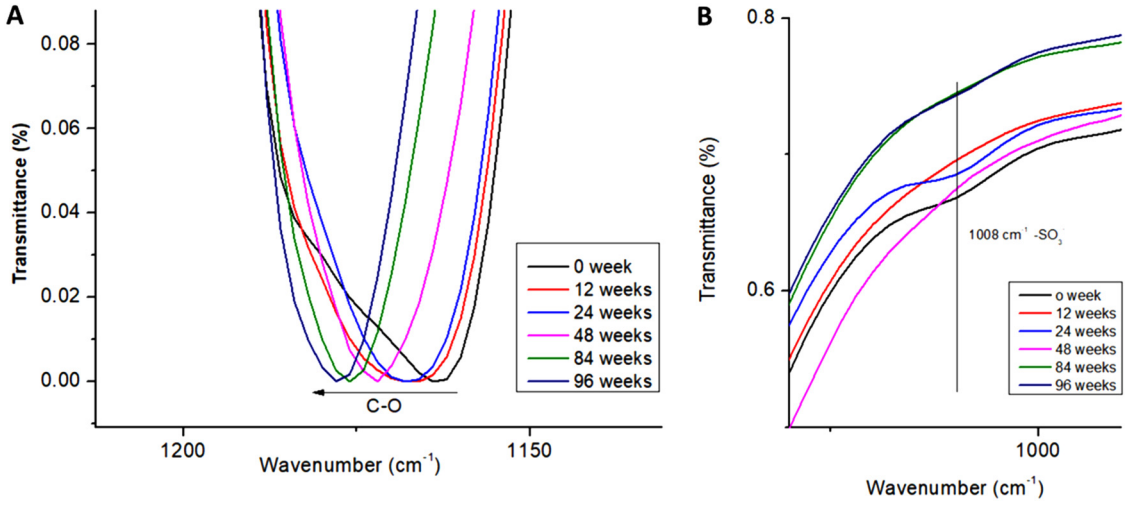

FIG. 10. (a) C—O—C peak of the FTIR spectrum showing the blueshift with degradation time for the grafted PCL samples degraded at 37 °C and (b) evolution of —SO_3^- groups on grafted-PCL films degraded at 37 °C over time.

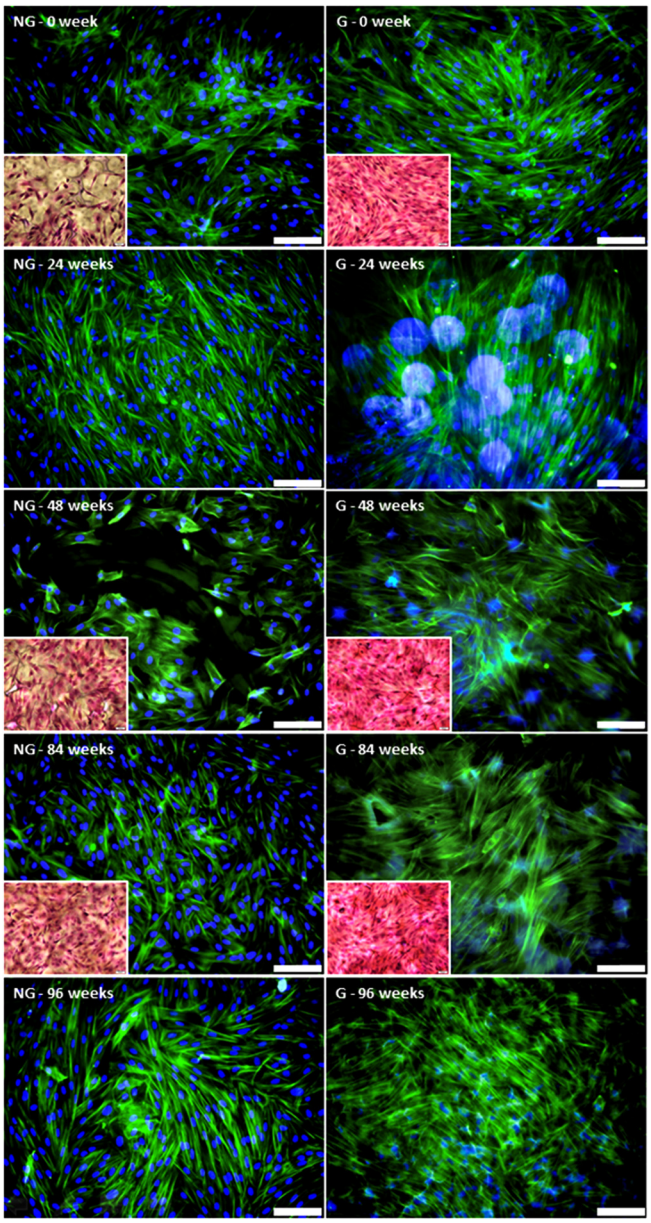

FIG. 11. Morphologies of sACL fibroblasts seeded for 7 days on nongrafted (NG) and grafted (G) PCL films degraded at 37 °C over the time period shown. Phalloidin (green)/DAPI (blue) labeling (scale bar = 100 μm) and H&E staining (insets).

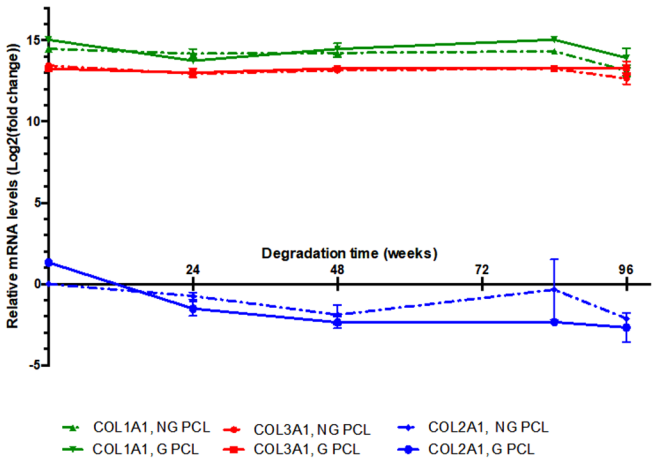

FIG. 12. RT-qPCR analysis of the expression levels of COL1A1, COL3A1, and COL2A1 genes in sheep ACL cells, cultured during 7 days, on nongrafted (NG) and grafted (G) PCL films degraded at 37 °C for 24, 48, 84, and 96 weeks. Graphs show means ± standard deviations of one to three samples of gene expression. The relative mRNA levels for each gene in the different experimental conditions were calculated as described in Sec. II. For all genes and experimental conditions, the COL2A1 values of NG PCL at T = 0 were used as control and normalized to 1. Consequently, all the relative mRNA levels are comparable between them. Cts of COL2A1, COL3A1 and COL1A1 were around 33 cycles, 20 cycles, and 19 cycles, respectively. COL2A1 was not expressed in the ACL cells, while COL3A1 and COL1A1 displayed high levels of expression in all the experimental conditions.

media weakens the intermolecular bonds, reducing the required tension to deform the fibers.[56] This decrease was less important for pNaSS grafted samples, since the grafting process has already "thermally treated" the fibers. On the other hand, grafted samples experienced a more severe increase in the crystallinity rate, which explains the more important elasticity reduction on the early stages of degradation. In these first weeks, an oscillation of UTS could also be noticed. This behavior can be linked to the combination of both of these phenomena and a nonhomogeneous degradation of the fibers in the bundle. After this point, the studied properties (E, ε, and σ_{max}) remained relatively stable until 24 weeks of degradation and then became noticeably modified by the degradation process (decreased E and σ_{max}; increased ε). In comparison to the native human ligament, after 96 weeks of natural static degradation the grafted fibers had higher rigidity (i.e., $E_{\text{PCL fibers, 96 weeks}} = 646 \pm 31$ MPa versus $E_{\text{native ligament}} = 114 \pm 53$ MPa) and ultimate stress (i.e., $\sigma_{\text{max (PCL fibers, 96 weeks)}} = 50.0 \pm 21.3$ MPa versus $\sigma_{\text{max (native ligament)}} = 24.5 \pm 11.2$ MPa). After 48 weeks of natural static degradation, the grafted fibers had higher elasticity (i.e., $\varepsilon_{\text{PCL fibers, 48 weeks}} = 15.7 \pm 1.4\%$ versus $\varepsilon_{\text{native ligament}} = 12.0 \pm 4.2\%$) than the native human ligament.

These bulk property analyses demonstrated that, even if the grafting accelerated the degradation kinetics of the PCL samples, the physico-chemical and mechanical properties were sufficiently stable for the first 6 months of natural degradation.

B. Surface analysis with degradation

The micro- and nano-topography observations were consistent with different modes of degradation between the grafted and nongrafted samples. The degraded nongrafted films exhibited holes in the amorphous regions, whereas the grafted films exhibited holes in the amorphous regions plus cracks in crystalline regions. Moreover,

at the nanoscale, the roughness increase in PCL surfaces after 120 weeks of degradation was lower on the grafted PCL films compared to nongrafted PCL films. These observations suggest conservation of pNaSS grafting over degradation time.

The contact angle measurements showed an increase of 28% in the hydrophilicity of the grafted films degraded at 37 °C for 120 weeks, which can explain why pNaSS grafting accelerated the degradation process after 6 months. Furthermore, the polar energy also increased over time, consistent with the surface segregation of polar groups linked to the PCL degradation.

Surface characterization demonstrated an increase of C—O species for all degradation conditions, consistent with the hydrolysis of the ester bonds of the PCL. These results were consistent with the degradation mechanism of the PCL described by Woodruff and Hutmacher.[33] Noteworthy, the molecular breakage was more gradual overtime on the pNaSS grafted surfaces compared to nongrafted. In the XPS sampling depth—around 100 Å depth—a decrease sulfur concentration over degradation time was observed, but trace amounts of sulfur were still detected on all degraded, grafted films. The colorimetric method commonly used to quantify the amount of sulfonate groups present could not be used due to high levels on nonspecific toluidine blue binding to the degraded polymer. The surface characterization at a deeper sampling depths by FTIR demonstrated a reduction of the C═O peak coupled with a blue shift of the C—O peak for all conditions over degradation time. These results were relevant for the PCL degradation process, which consists of the cutting of the ester bonds and was accelerated by the increase in the degradation temperature as well as pNaSS grafting. Finally, the FTIR analysis, which probes deeper into the sample than XPS, detected the presence of pNaSS after long-term degradation confirming the pNaSS grafting remains after long-term natural degradation.

C. Biological impact of degraded materials

The cytotoxicity experiments confirmed the absence of *in vitro* cytotoxicity from the PCL degradation products, as has been reported in the literature[57] but also demonstrated no cytotoxicity from the degradation products from the pNaSS grafted surface. The cell morphology study showed that cells still have the ability to grow on the degraded surfaces, which likely was amplified by the increased surface roughness produced by the degradation process.[58,59] Moreover, it has been already demonstrated that pNaSS grafting can modulate the fibroblast morphology, adhesion, and activity.[22,27] With the morphology images presented in this article, we observed that the improvement in cell spreading due to pNaSS grafting still present for degradation times up almost 2 yr. This result confirmed the effect of pNaSS and its presence over the long-term natural degradation as observed by AFM, XPS, FTIR, and contact angles. Finally, the collagen gene expression reveled that primary ligament cells did not lose their phenotype when in contact with degraded surface: they maintained a high and stable type-I and -III collagen gene expression without significant differences between nongrafted and grafted surfaces. In contrast, the type-II collagen gene, corresponding to the cartilage lineage, did not appear to be expressed in primary ligament cells.

V. CONCLUSION

This study evaluated the long-term hydrolytic degradation of two different types of PCL (films and fibers) with different microstructures and molecular weights (i.e., films: $M_n = 60\,614 \pm 743$ g mol^{-1} and spherulites structure versus fiber bundles: $M_n = 74\,674 \pm 2438$ g mol^{-1} and shish-kebab structure). The obtained results confirmed the literature reports that PCL hydrolyzes by a bulk degradation mode with increasing degradation kinetics for lower molecular weights and higher degradation temperatures.[11,36,60,61]

Nevertheless, the aim of this study was to evaluate the impact of the pNaSS grafting on the long-term PCL degradation process. The obtained results showed a strong difference in the kinetics of the degradation process. While PCL surfaces follows the extensively described process of PCL degradation that depends on molecular weight, crystallinity, and temperature,[33] in the case of the pNaSS grafted samples, degradation still depends on the same parameters, but the presence of grafted pNaSS macromolecular chains increases the hydrophilic properties of the PCL surfaces, which in turn strongly accelerates the surface degradation process. To address the question "would the mechanical properties of pNaSS grafted PCL fibers be enough strong to act as a ligament prosthesis after long term degradation?," the results from this study show that the ultimate shear stress of the degraded fibers after 96 weeks is higher than the ultimate shear stress of the natural ligament.

ACKNOWLEDGMENTS

This work was funded as part of the "Future Investment Project" by the French Public Investment Bank and the French state—PSPC application—Liga2bio project (V.M.). The XPS experiments done at NESAC/Bio were supported by the National Institutes of Health (NIH) Grant (No. EB-002027). We would like to thank Gerry Hammer (NESAC/Bio) for his technical help with the XPS analysis and Laila Farias-Colaco for her technical help on mechanical testing.

REFERENCES

[1]H. Sun, L. Mei, C. Song, X. Cui, and P. Wang, Biomaterials **27**, 1735 (2006).
[2]F. A. Petrigliano, G. A. Arom, A. N. Nazemi, M. G. Yeranosian, B. M. Wu, and D. R. McAllister, Tissue Eng. Part A **21**, 1228 (2015).
[3]C. P. Laurent, D. Durville, D. Mainard, J.-F. Ganghoffer, and R. Rahouadj, J. Mech. Behav. Biomed. Mater. **12**, 184 (2012).
[4]H. M. Pauly, D. J. Kelly, K. C. Popat, N. A. Trujillo, N. J. Dunn, H. O. McCarthy, and T. L. H. Donahue, J. Mech. Behav. Biomed. Mater. **61**, 258 (2016).
[5]A. C. Gurlek, B. Sevinc, E. Bayrak, and C. Erisken, Mater. Sci. Eng. C **71**, 820 (2017).
[6]Z. X. Meng, W. Zheng, L. Li, and Y. F. Zheng, Mater. Sci. Eng. C **30**, 1014 (2010).
[7]X. Jing, H.-Y. Mi, T. M. Cordie, M. R. Salick, X.-F. Peng, and L.-S. Turng, Polymers **55**, 5396 (2014).
[8]S. Abbaspoor, S. Agbolaghi, and F. Abbasi, Eur. Polym. J. **103**, 293 (2018).
[9]C. X. Lam, S. H. Teoh, and D. W. Hutmacher, Polym. Int. **56**, 718 (2007).
[10]A. Höglund, M. Hakkarainen, and A. Albertsson, J. Macromol. Sci. Part A **44**, 1041 (2007).
[11]L. A. Bosworth and S. Downes, Polym. Degrad. Stab. **95**, 2269 (2010).
[12]O. Hartman, C. Zhang, E. L. Adams, M. C. Farach-Carson, N. J. Petrelli, B. D. Chase, and J. F. Rabolta, Biomaterials **31**, 5700 (2010).

[13]J. M. Miszuk, T. Xu, Q. Yao, F. Fang, J. D. Childs, Z. Hong, J. Tao, H. Fong, and H. Sun, Appl. Mater. Today **10**, 194 (2018).
[14]J. S. Stevens, A. C. de Luca, S. Downes, G. Terenghi, and S. L. M. Schroeder, Surf. Interface Anal. **46**, 673 (2014).
[15]G. Amokrane, C. Falentin-Daudré, S. Ramtani, and V. Migonney, IRBM **39**, 268 (2018).
[16]L. A. Can-Herrera, A. Ávila-Ortega, S. de la Rosa-García, A. I. Oliva, J. V. Cauich-Rodríguez, and J. M. Cervantes-Uc, Eur. Polym. J. **84**, 502 (2016).
[17]M. Asadian *et al.*, ACS Appl. Mater. Interfaces **10**, 41962 (2018).
[18]C. Latz, G. Pavon-Djavid, G. Hélary, M. D. Evans, and V. Migonney, Biomacromolecules **4**, 766 (2003).
[19]P. Yammine, G. Pavon-Djavid, G. Helary, and V. Migonney, Biomacromolecules **6**, 2630 (2005).
[20]F. Anagnostou, A. Debet, G. Pavon-Djavid, Z. Goudaby, G. Hélary, and V. Migonney, Biomaterials **27**, 3912 (2006).
[21]M. Ciobanu, A. Siove, V. Gueguen, L. J. Gamble, D. G. Castner, and V. Migonney, Biomacromolecules **7**, 755 (2006).
[22]J. Zhou, M. Ciobanu, G. Pavon-Djavid, V. Gueguen, and V. Migonney, Proc. IEEE Eng. Med. Biol. **29**, 5115 (2007).
[23]G. Pavon-Djavid, L. J. Gamble, M. Ciobanu, V. Gueguen, D. G. Castner, and V. Migonney, Biomacromolecules **8**, 3317 (2007).
[24]S. Lessim, V. Migonney, P. Thoreux, D. Lutomski, and S. Changotade, Biomed. Mater. Eng. **4**, 289 (2013).
[25]V. Viateau, J. Zhou, S. Guérard, M. Manassero, M. Thourot, F. Anagnostou, D. Mitton, B. Brulez, and V. Migonney, IRBM **32**, 118 (2011).
[26]J. Zhou, M. Manassero, V. Migonney, and V. Viateau, IRBM **30**, 153 (2009).
[27]C. Vaquette, V. Viateau, S. Guérard, F. Anagnostou, M. Manassero, D. G. Castner, and V. Migonney, Biomaterials **34**, 7048 (2013).
[28]S. Huot, G. Rohman, M. Riffault, A. Pinzano, L. Grossin, and V. Migonney, Biomed. Mater. Eng. **4**, 281 (2013).
[29]N. Djaker, S. Brustlein, G. Rohman, S. Huot, M. L. de la Chapelle, and V. Migonney, Biomed. Opt. Express **5**, 149 (2014).
[30]G. Rohman, S. Huot, M. Vilas-Boas, G. Radu-Bostan, D. G. Castner, and V. Migonney, J. Mater. Sci. Mater. Med. **26**, 5539 (2015).
[31]A. Leroux, C. Egles, and V. Migonney, PLoS One **13**, 205722 (2018).
[32]A. Leroux, E. Maurice, V. Viateau, and V. Migonney, IRBM **40**, 38 (2019).
[33]M. A. Woodruff and D. W. Hutmacher, Prog. Polym. Sci. **35**, 1217 (2010).
[34]T. Ivanova, N. Grozev, I. Panaiotov, and J. E. Proust, Colloid Polym. Sci. **277**, 709 (1999).
[35]Sandra Sánchez-González, Nazely Diban, and Ane Urtiaga, Membranes **8**, 12 (2018).
[36]C. X. F. Lam, M. M. Savalani, S.-H. Teoh, and D. W. Hutmacher, Biomed. Mater. **3**, 034108 (2008).
[37]H.-J. Sung, C. Meredith, C. Johnson, and Z. S. Galis, Biomaterials **25**, 5735 (2004).
[38]A. C. Vieira, J. C. Vieira, J. M. Ferra, F. D. Magalhães, R. M. Guedes, and A. T. Marques, J. Mech. Behav. Biomed. Mater. **4**, 451 (2011).
[39]I. Castilla-Cortázar, J. Más-Estellés, J. M. Meseguer-Dueñas, J. L. Escobar Ivirico, B. Marí, and A. Vidaurre, Polym. Degrad. Stab. **97**, 1241 (2012).
[40]D. C. França, E. B. Bezerra, D. D. de S. Morais, E. M. Araújo, and R. M. R. Wellen, Mater. Res. **19**, 618 (2016).
[41]G. P. Sailema-Palate, A. Vidaurre, A. J. Campillo-Fernández, and I. Castilla-Cortázar, Polym. Degrad. Stab. **130**, 118 (2016).
[42]D. C. França, D. D. Morais, E. B. Bezerra, E. M. Araújo, and R. M. R. Wellen, Mater. Res. **21**, e20170837 (2018).
[43]H. Samami and J. Pan, J. Mech. Behav. Biomed. Mater. **59**, 430 (2016).
[44]K. Sevim and J. Pan, Acta Biomater. **66**, 192 (2018).
[45]Q. Zhang, Y. Jiang, Y. Zhang, Z. Ye, W. Tan, and M. Lang, Polym. Degrad. Stab. **98**, 209 (2013).
[46]G. Liao, S. Jiang, X. Xu, and Y. Ke, Mater. Lett. **82**, 159 (2012).
[47]P. S. P. Poh, D. W. Hutmacher, B. M. Holzapfel, A. K. Solanki, and M. A. Woodruff, Data Brief **7**, 923 (2016).
[48]Y. Shi, J. Liu, L. Yu, L. Z. Zhong, and H. B. Jiang, Ceram. Int. **44**, 15086 (2018).
[49]M. Marrese, V. Cirillo, V. Guarino, and L. Ambrosio, J. Funct. Biomater. **9**, 27 (2018).
[50]M. A. Basile, G. G. d'Ayala, M. Malinconico, P. Laurienzo, J. Coudane, B. Nottelet, F. DellaRagione, and A. Oliva, Mater. Sci. Eng. C **48**, 457 (2015).
[51]L. Ghasemi-Mobarakeh, M. P. Prabhakaran, M. Morshed, M. H. Nasr-Esfahani, and S. Ramakrishna, Mater. Sci. Eng. C **30**, 1129 (2010).
[52]H. Y. Kweon, M. K. Yoo, I. K. Park, T. H. Kim, H. C. Lee, H. Lee, J. Oh, T. Akaike, and C. Cho, Biomaterials **24**, 801 (2003).
[53]L. Goebel, P. Orth, M. Cucchiarini, D. Pape, and H. Madry, Osteoarthr. Cartilage **25**, 581 (2017).
[54]K. J. Livak and T. D. Schmittgen, Methods **25**, 402 (2001).
[55]B. Nie, J. Stutzman, and A. Xie, Biophys. J. **88**, 2833 (2005).
[56]A. Rangel, L. Colaço, N. T. Nguyen, J.-F. Grosset, C. Egles, and V. Migonney, IRBM (published online) (2020).
[57]S. C. Woodward, P. S. Brewer, F. Moatamed, A. Schindler, and C. G. Pitt, J. Biomed. Mater. Res. **19**, 437 (1985).
[58]D. D. Deligianni, N. Katsala, S. Ladas, D. Sotiropoulou, J. Amedee, and Y. F. Missirlis, Biomaterials **22**, 1241 (2001).
[59]E. Rosqvist, E. Niemelä, A. P. Venu, R. Kummala, P. Ihalainen, M. Toivakka, J. E. Eriksson, and J. Peltonen, Colloids Surf. B Biointerfaces **174**, 136 (2019).
[60]C. G. Pitt, F. I. Chasalow, Y. M. Hibionada, D. M. Klimas, and A. Schindler, J. Appl. Polym. Sci. **26**, 3779 (1981).
[61]T. Sekiguchi *et al.*, Polym. Degrad. Stab. **96**, 1397 (2011).
[62]See supplementary material at https://doi.org/10.1116/6.0000429 for more information on PCL fiber degradation and films contact angle.